Dynamics-Function Correlation in Cu, Zn Superoxide Dismutase: A Spectroscopic and Molecular Dynamics Simulation Study

M. Falconi,* M. E. Stroppolo,* P. Cioni,† G. Strambini,† A. Sergi,‡ M. Ferrario,§ and A. Desideri*
*INFM and Department of Biology, University of Rome "Tor Vergata", Via della Ricerca Scientifica, 00133, Rome, Italy. †Istituto di Biofisica CNR, Pisa; ‡INFM and Department of Physics, University of Rome "La Sapienza", 00185 Rome; and §INFM Department of Physics, University of Modena, 41100 Modena, Italy.

ABSTRACT A single mutation (Val29→Gly) at the subunit interface of a Cu, Zn superoxide dismutase dimer leads to a twofold increase in the second order catalytic rate, when compared to the native enzyme, without causing any modification of the structure or the electric field distribution (Stroppolo et al., 2000). To check the role of dynamic processes in this catalytic enhancement, the flexibility of the dimeric protein at the subunit interface region has been probed by the phosphorescence and fluorescence properties of the unique tryptophan residue. Multiple spectroscopic data indicate that Trp83 experiences a very similar, and relatively hydrophobic, environment in both wild-type and mutant protein, whereas its mobility is distinctly more restrained in the latter. Molecular dynamics simulation confirms this result, and provides, at the molecular level, details of the dynamic change felt by tryptophan. Moreover, the simulation shows that the loops surrounding the active site are more flexible in the mutant than in the native enzyme, making the copper more accessible to the incoming substrate, and being thus responsible for the catalytic rate enhancement. Evidence for increased, dynamic copper accessibility also comes from faster copper removal in the mutant by a metal chelator. These results indicate that differences in dynamic, rather than structural, features of the two enzymes are responsible for the observed functional change.

INTRODUCTION

It is generally accepted that protein structure is closely related to function. However, in some cases, structure alone cannot explain the functional properties of an enzyme if its dynamic features are not taken into account. Reactions involving macromolecules are often highly dependent on excursions to excited molecular conformations, and, hence, are intimately coupled to the structural flexibility. Up to now, however, there are just few clear examples in which the dynamics/function correlation is unequivocally demonstrated (Kay, 1998; Kohen et al., 1999).

Here we report the example of Cu, Zn superoxide dismutase (SOD), in which the electron transfer mechanism between the substrate and the active site is considered to have reached perfection because the second order catalytic rate is limited by diffusion (Bordo et al., 2001). Actually, the steering of the negatively charged substrate is enhanced through an appropriate distribution of the electrostatic field around the protein (Klapper et al., 1986; Sines et al., 1990), which, in the eukaryotic enzymes, is conserved among different species (Desideri et al., 1992). This distribution provides a constant high substrate-enzyme association rate and second-order catalytic rate k_{cat}/K_M (Sergi et al., 1994; O'Neill et al., 1988). An analogous electrostatic mechanism is also operative with prokaryotic Cu, Zn SODs that, although maintaining the typical β-barrel fold of the subunit structure, show different quaternary structure assembly and a different location of the electrostatic loop, when compared to the eukaryotic enzyme (Bourne et al., 1996; Bordo et al., 1999). In fact, rational single mutations of charged amino acid residues yielded prokaryotic mutants that had a higher catalytic rate than the native enzyme (Folcarelli et al., 1999).

Recently we have shown that the second order catalytic rate of *Photobacterium leiognathi* Cu, Zn SOD (PSOD) increases by two times upon mutation of the uncharged amino acid Val29 (Fig. 1), located at the subunit interface, into glycine (Stroppolo et al., 2000). Interestingly such a mutation does not produce any significant structural change. In particular, the structure of the copper active site is fully conserved, as evidenced by x-ray comparative analysis of the native and mutant structures (Stroppolo et al., 2000), making it difficult to explain the increased catalytic rate. We presently have evidence, obtained through spectroscopic techniques and molecular dynamics (MD) simulation, that the main effect of the mutation is to modify the dynamic behavior of the enzyme structure, thus providing a clear example of dynamics-function relationship.

MATERIALS AND METHODS

Sample preparation

Single site mutant Val29→Gly of the recombinant Cu, Zn PSOD was prepared in a two step PCR approach (Landt et al., 1990). The amplified DNA was restricted with *Eco*RI and *Hin*dIII, and subsequently cloned into vector pEMBL18 that was previously digested with the same restriction enzymes. The expression plasmid obtained was inserted into the *Escherichia coli* strain DH5α, as well as for wild-type PSOD. Recombinant clones were grown in standard LB medium containing AMP (70 μg/ml) for

Received for publication 10 October 2000 and in final form 20 March 2001.

Address reprint requests to A. Desideri, Department of Biology, University of Rome "Tor Vergata", Via della Ricerca Scientifica, 00133, Rome, Italy. Phone: 39 0672594376; Fax: 39 0672594326; E-mail: desideri@uniroma2.it.

0006-3495/01/06/2556/12 $2.00

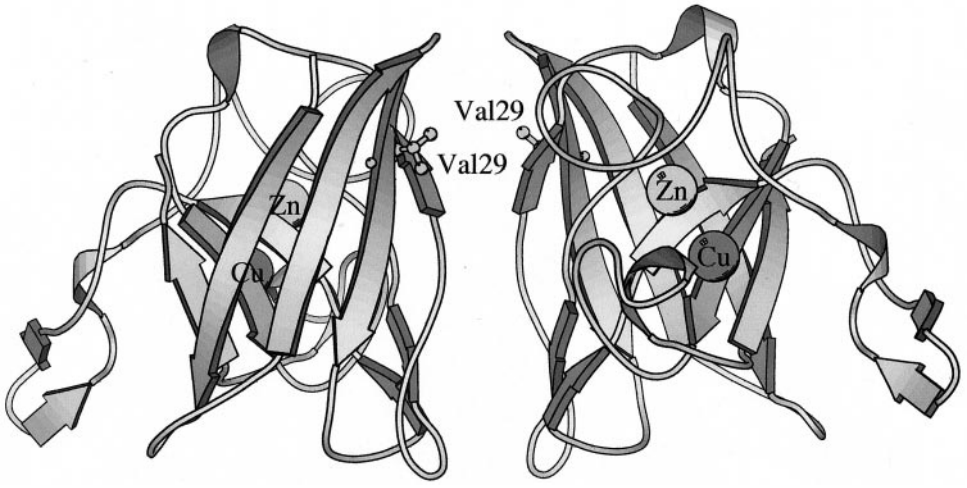

FIGURE 1 *Photobacterium leiognathi* Cu, Zn SOD structure. Arrows represent the β-strands while thin wires represent the random-coil structure and the turns. The copper and the zinc ions are shown as labeled spheres. Residue Val29, mutated in glycine, is represented as a ball-and-stick model. This picture has been obtained using the program Molscript (Kraulis, 1991).

6 h at 37°C. Then 0.25 mmol of $CuSO_4$ and 80 μmol of $ZnSO_4$ were added, and the cells were left to grow for another 2 h. Proteins were extracted and purified as previously described (Foti et al., 1997). Proteins were purified to 98%, as judged by sodium dodecyl sulfate-polyacrylamide gel electrophoresis. Protein concentration was evaluated by the method of Lowry (Lowry et al., 1951), using bovine serum albumin as standard. Selective removal of Cu^{2+} to produce copper-free PSOD was carried out as reported before (Calabrese et al., 1976). Copper content was evaluated by double integration of the EPR spectra, using a Cu^{2+}- EDTA solution as standard and by atomic absorption using a Perkin-Elmer 3030 spectrometer equipped with a graphite furnace.

The effect of EDTA on the activity of wild-type and mutated PSOD was analyzed as previously described (Battistoni et al., 1998). Cu, Zn PSOD samples, at a concentration of 0.04 mg/ml, were incubated at 37°C in 10 mM phosphate buffer, 0.1 mM EDTA (pH 7.3). Aliquots were withdrawn at different times, and immediately assayed for residual activity by the pyrogallol method (Marklund and Marklund, 1974).

Spectroscopic grade propylene glycol was from Merck (Darmstadt, Germany) and was treated with reducing agent ($NaBH_4$) and distilled under vacuum before use. Water, doubly distilled over quartz, was purified by a Milli-Q Plus system (Millipore Corporation, Bedford, MA). All glassware used for sample preparation was conditioned in advance by storage for 24 h in 10% HCl Suprapur (Merck). For phosphorescence measurements in fluid solutions, it is paramount to eliminate all traces of O_2. For phosphorescence lifetime measurements, the samples were placed in 5 $\times$ 5 mm square quartz cuvettes that were specially designed to allow thorough removal of O_2 by the alternative application of moderate vacuum and inlet of ultra pure N_2 (Strambini and Gonnelli, 1995). In all phosphorescence experiments the concentration of protein was 5 μM.

Phosphorescence and fluorescence spectroscopy

Routine fluorescence spectra and steady-state anisotropy were recorded using a photon-counting spectrofluorimeter (Model K2 ISS Champaign, IL). A conventional homemade instrumentation was employed for all phosphorescence intensity, spectra and lifetime measurements in low temperature glasses. The excitation provided by a Cermax xenon lamp (LX 150 uv; ILC Technology, Sunnyvale, CA) was selected by a 0.25 m grating monochromator (Jobin-Yvon, H25, Longjumeau, France) and the emission, dispersed by another 0.25 m grating monochromator (Jobin-Yvon, H25), was detected with an EMI 9635 QB photomultiplier. Phosphorescence decays in fluid solutions were measured on an apparatus that was previously described (Strambini and Gonnelli, 1995). Briefly, pulsed excitation was provided by a frequency-doubled flash-pumped dye laser (UV 500 M-Candela) (λ_{ex} = 292 nm) with a pulse duration of 1 μs and energy per pulse of typically 1 to 10 mJ. The emitted light was collected at 90° from the excitation direction and selected by a filter combination with a transmission window between 420 and 460 nm. The photomultiplier was protected from the intense excitation and fluorescence light pulse by a high-speed chopper blade that closed the slits during laser excitation. The minimum dead time of the apparatus is about 10 μs. All the decaying signals were digitized and averaged with a computerscope system (EGAA; RC Electronics). Subsequent analysis of decay curves in terms of discrete exponential components was carried out by a nonlinear least squares fitting algorithm, implemented by the program Global Analysis (Global Unlimited, LFD University of Illinois, Urbana, IL). All reported decay data are averages of three or more independent measurements. The reproducibility of τ_p was typically better than 5%. Acrylamide quenching experiments were carried out as described before (Cioni and Strambini, 1998). The phosphorescence emission of SOD is intrinsically heterogeneous and remains so even when the average phosphorescence lifetime is considerably reduced by acrylamide. Such lifetime heterogeneity reflects multiple stable conformations of the macromolecule, each with its distinct intrinsic phosphorescence lifetime and acrylamide quenching rate constant. For convenience, lifetime Stern-Volmer plots were all constructed from the average lifetimes, $\tau_{av} = \Sigma\alpha_i\tau_i$, obtained in general from a biexponential fit of phosphorescence decays. Consequently, the value of k_q, which reports the diffusion coefficient of acrylamide into the macromolecule, derived from these plots is an averaged quantity.

COMPUTATIONAL METHODS

Molecular dynamics

The coordinates of the wild-type PSOD at 2.1 Å resolution (Bordo et al., 1999) were obtained from the RCSB Protein Data Bank (Berman et al., 2000) (entry code 1BZO). The coordinates of the mutant were kindly provided by Professor M. Bolognesi (Stroppolo et al., 2000). For sake of clarity in this work, the sequential numbering of the PSOD chain (from Gln1 to Gln151) applied by Bourne and collaborators (Bourne et al., 1996), has been used. A 1.4-ns trajectory of molecular dynamics simulation of the native and mutant enzymes have been performed on an SGI Origin 200, by considering the dimeric proteins embedded in 5494 and 5602 water molecules, respectively. The total number of atoms for the two systems were 19,176 for the wild-type and 19,494 for the mutant. No counterions were needed due to the neutral charge of both the systems. Periodic boundary conditions (Allen and Tildesley, 1987) have been used. The equilibrium

properties of solvated dimers were sampled in the isothermal-isobaric ensemble (Melchionna and Ciccotti, 1997). The temperature chosen for our study was 300 K, and pressure was kept fixed at 1.0 atm. The MD integration time step was 1.0 fs. The simulation was performed using the computer code DL-PROTEIN (Smith and Forester, 1996; Melchionna et al., 1998). We used the GROMOS (van Gunsteren and Berendsen, 1987) force field with the set of parameters denoted "37c" and the water molecules represented by means of the SPC/E model (Berendsen et al., 1987). All bond lengths were kept fixed over time by using the SHAKE iterative procedure (Ryckaert et al., 1977). Electrostatic interactions were carefully computed using the Ewald sum method (Allen and Tildesley, 1987).

The dynamic behaviors of these proteins in the MD simulation have been analyzed by using the dynamic cross-correlation map (DCCM) to yield information about possible correlated motions (McCammon and Harvey, 1987). Correlated motions can occur between residues belonging to the same or to different subunits. The extent of correlated motions between residues is indicated by the magnitude of the corresponding correlation coefficient between their C_α atoms. The cross-correlation coefficient for the displacement of each pair of C_α atoms *i* and *j* is given by:

$$c_{ij} = \frac{\langle \Delta \mathbf{r}_i \cdot \Delta \mathbf{r}_j \rangle}{\sqrt{\langle \Delta \mathbf{r}_i^2 \rangle \langle \Delta \mathbf{r}_j^2 \rangle}} \quad (1)$$

where $\Delta \mathbf{r}_i$ is the displacement from the mean position of the *i*th atom and the $\langle\ \rangle$ represent the time average over the whole trajectory.

RESULTS AND DISCUSSION

Spectroscopic analysis

Tryptophan phosphorescence and fluorescence spectroscopy was utilized to investigate both structural and dynamic features of PSOD in solution, by taking advantage of the single Trp83 residue placed at the dimer subunit interface. All the phosphorescence properties reported here refer to the copper-free enzyme, as the metal ion bound at the active site was found to completely quench the phosphorescence emission of Trp83. Addition of copper to the copper-free protein gave a protein indistinguishable from the native one, allowing us to safely use the phosphorescence data to compare structural/dynamic differences between the native and mutated enzyme.

Information on the Trp environment can be obtained from the high-resolution phosphorescence spectrum, the phosphorescence lifetime, and the accessibility of the indole ring to interactions with external solutes. The low temperature (140 K) phosphorescence spectrum of mutant PSOD is reported in Fig. 2. The peak wavelength ($\lambda_{0,0}$) of the 0,0 vibronic band, related to the polarity of the Trp environment, is 409.5 nm. Compared to values of 406 to 407 nm, typical for residues fully exposed to the solvent, this wavelength is red-shifted and characteristic of a largely hydrophobic environment (Hershberger et al., 1980). The band is only slightly blue-shifted (0.5 nm) compared to wild-type PSOD (Fig. 2, *inset*), and therefore indicates that in the mutant protein, the chemical nature of the protein structure in proximity of the aromatic ring is essentially the same as in the native enzyme. The bandwidth of the 0,0 vibronic band, the parameter normally taken to indicate the resolution of the spectrum, provides information on the structural homogeneity of the Trp environment. The bandwidth is 5.5 nm for the Val29→Gly and 4.8 nm for the wild-type protein (Fig. 2, inset). In both cases it is larger than the 3.9 nm expected for a homogeneous site (see reference spectrum included in Fig. 2; Gabellieri et al., 1996), demonstrating a certain degree of structural heterogeneity in the SOD dimer that is more pronounced in the mutant protein.

The phosphorescence lifetime in the low temperature glass is unaffected by the mutation being 6.2 and 6.1 s for the wild-type and mutant protein, respectively (Fig. 3 *A*). Lifetimes around 6 s are characteristic of Trp residues not perturbed by the proximity of disulfides or other quenching groups, a finding that is consistent with the 3D structure of these proteins (Bordo et al., 1999). The phosphorescence lifetime is shortened by the heavy-atom perturbation induced by addition of iodide as shown in Fig. 3. The phosphorescence of PSOD in the presence of 1 M I^- decays rapidly, at variance of what happens in presence of 1 M Cl^-, and in a highly non-exponential fashion, indicating that Trp83 is within 5 Å from I^- atoms randomly distributed in the solvent (Lee, 1985). The interaction is stronger in the mutant protein (Fig. 3 *C*) than in the native one (Fig. 3 *B*) suggesting that as a result of the mutation Trp83 is more accessible to the perturbing agent.

A clear distinction between the two proteins, in terms of their structural flexibility at the subunit interface region, is revealed by the phosphorescence lifetime in fluid media. The phosphorescence decay in buffer at 274 K (Fig. 4) shows that the mutation has caused an increase of the intrinsic lifetime, implying that the local structure has become more rigid. It should also be noted that, in both proteins, the decay is non-exponential and requires two lifetime components to adequately fit the data. The resulting lifetimes are $\tau_1 = 56$ and $\tau_2 = 28$ ms for the mutated and $\tau_1 = 44$ ms and $\tau_2 = 20$ ms for the native enzyme, respectively. The amplitudes of the populations are $\alpha_1 = \alpha_2 = 0.5$ in both cases. For a protein with a single Trp residue, the observation of different lifetimes provides a clear evidence of conformational heterogeneity (Cioni et al., 1994) because it indicates that the conformers of PSOD are nonequivalent in the dynamic properties of the Trp environment, when averaged over a time window of the order of τ. The empirical correlation between the intrinsic lifetime and the solution viscosity, established with model compounds (Strambini and Gonnelli, 1985, 1995), allows an estimate of the local effective viscosity of the two main conformers. They correspond to 1079 and 438 cP in the mutated and 806 and 264 cP in the native protein, respectively. The rigidity at the subunit interface increases in the mutant protein, indicating small local rearrangements likely due to additional bonding interactions around Trp83.

In addition to the intrinsic lifetime, the flexibility of globular proteins can be investigated by monitoring the diffusion of small quenching molecules through the protein

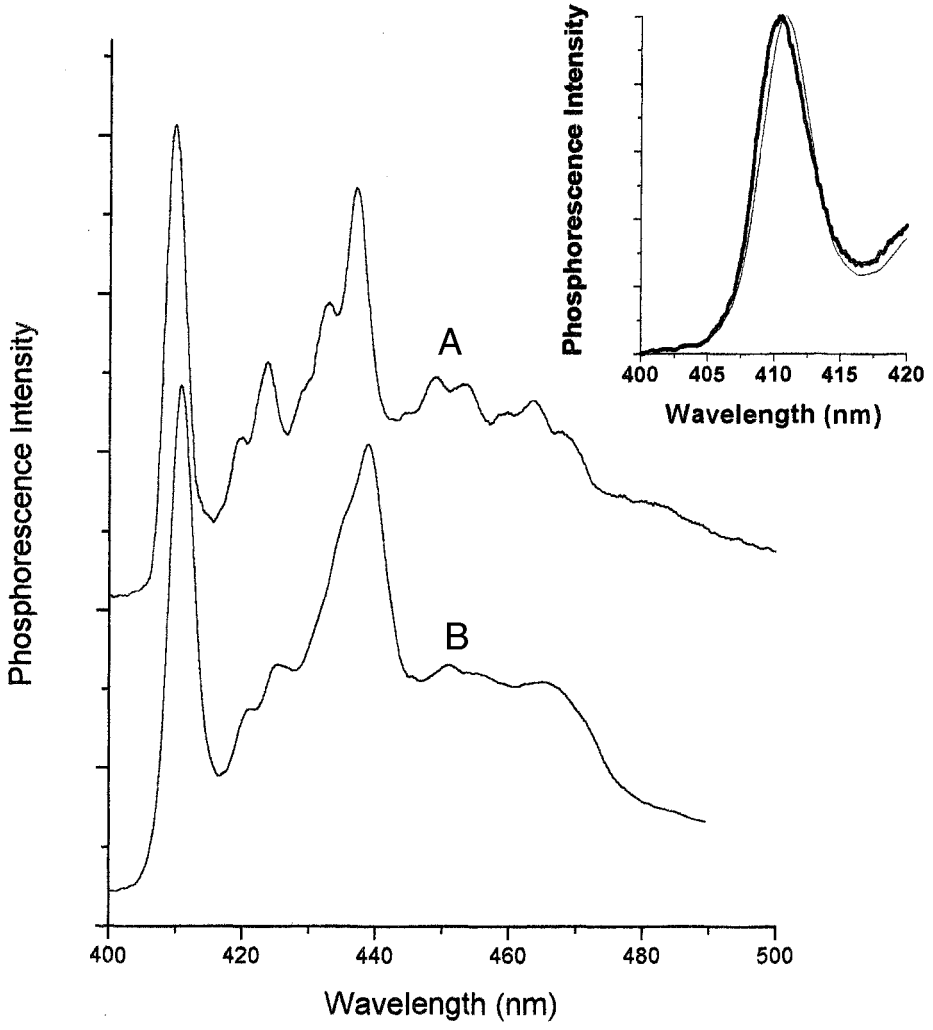

FIGURE 2 Phosphorescence spectrum, of Trp84 of glyceraldehyde-3-phosphate dehydrogenase (Gabellieri et al., 1996) (*A*), included as reference for the phosphorescence spectrum of Val29→Gly PSOD in a propylene glycol/buffer (50/50, V/V) glass at 140 K (*B*). (*Inset*) comparison of the 0,0 vibrational band of the spectrum of wild-type (*thin line*) and of Val29→Gly mutant (*heavy line*) PSOD. The protein concentration is 5 μM in 10 mM phosphate buffer (pH 7.5). The excitation wavelength is 295 nm.

matrix to the phosphorescent chromophore. In particular, quenching of protein phosphorescence by acrylamide was shown to be a sensitive indicator of the protein overall flexibility (Cioni and Strambini, 1998). The bimolecular quenching rate constant, k_q, derived from the lifetime Stern-Volmer plot ($1/\tau = 1/\tau_0 + k_q$ [acrylamide], τ_0 being the unperturbed lifetime) provides a measure of the acrylamide diffusion coefficient inside the macromolecule. The magnitude of k_q was found to be $1.4 \pm 0.2 \times 10^4$ M^{-1} s^{-1} for both the wild-type and mutant protein, indicating that the average overall flexibility of the protein is very similar in both cases.

The fluorescence properties of Trp are also diagnostic of an unchanged structure in the mutated protein but of different dynamics. In fact, both fluorescence intensity and emission wavelength of the mutant are identical to those observed in the protein, confirming a relatively hydrophobic although still water accessible, Trp environment (Malvezzi-Campeggi et al., 1999). On the other hand, the steady-state anisotropy in the mutant is distinctly larger than in the native enzyme (0.137 ± 0.003 against 0.125 ± 0.002); the inhibition of independent indole ring rotations confirms that the mutation has rendered the local structure more rigid.

Overall spectroscopic data suggest that differences between native and mutated enzymes, as monitored by the Trp probe located at the inter-subunit surface, are relegated mostly to their dynamic properties rather than to specific, static structural changes.

Molecular dynamics simulations

To investigate further the different dynamic properties of the two enzymes we have carried out state of the art MD simulations (trajectory lengths, 1.4 ns) of both the native and Val29→Gly proteins. Fig. 5 reports a series of structural parameters (Kabsch and Sander, 1983) monitored during the trajectory for both native and mutated proteins. The data indicate that the structure of the two proteins is conserved over all of the trajectory, and that

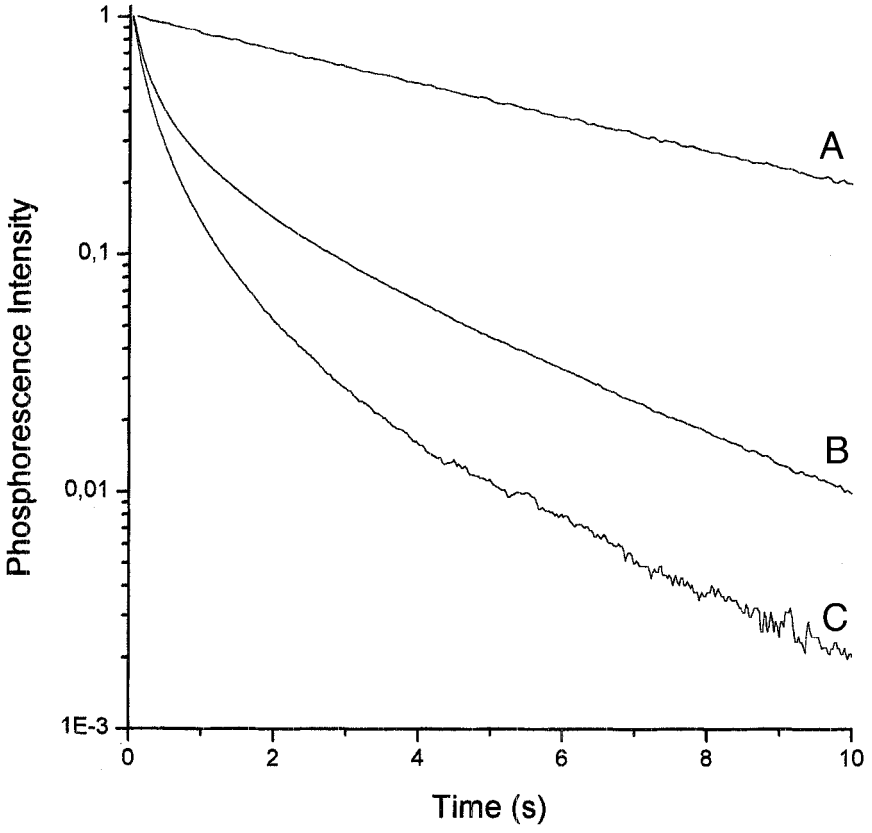

FIGURE 3 Phosphorescence decay at 140 K of wild-type PSOD in presence of 1 M KCl (*A*), the same decay is observed for the Val29→Gly mutant. Phosphorescence decay of wild-type (*B*) and Val29→Gly (*C*) PSOD in presence of 1 M KI. Protein conditions are as in Fig. 2.

both are sampling conformations close to their native 3D structure (Fig. 5 *A–D*). Notwithstanding, in each protein, the two subunits behave in a different way, and changes are found in the relationship between the monomers. In fact, the x-ray structure of the mutant indicates that the volume between the two subunits is smaller than in the native enzyme (Stroppolo et al., 2000). In particular the volume between the two subunits, including inter-subunit

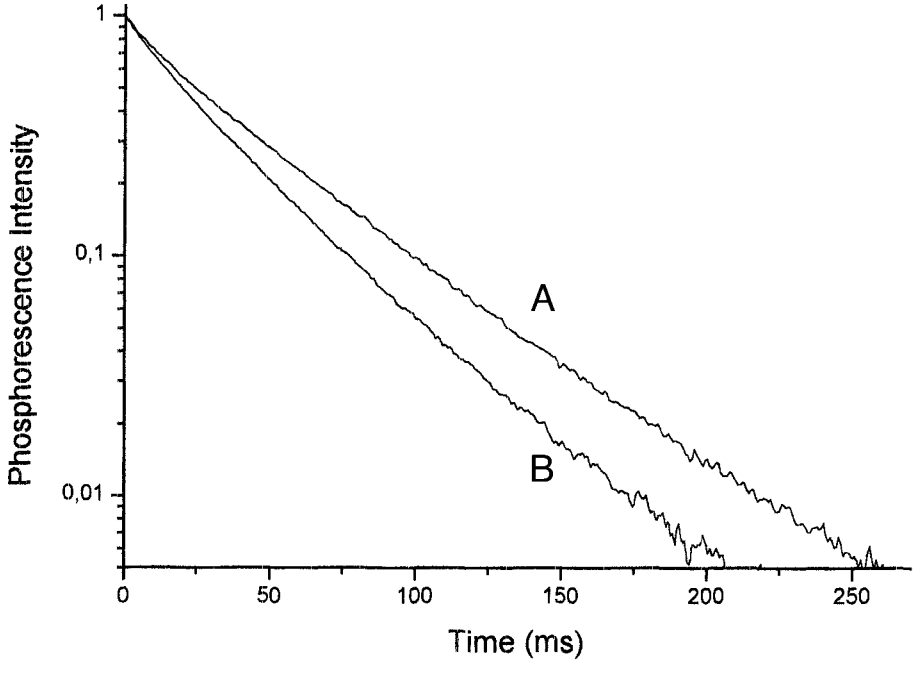

FIGURE 4 Phosphorescence decays of Val29→Gly mutant (*A*); and of wild-type (*B*) PSOD, at 274 K. The protein concentration is 5 μM in 10 mM phosphate buffer (pH 7.5).

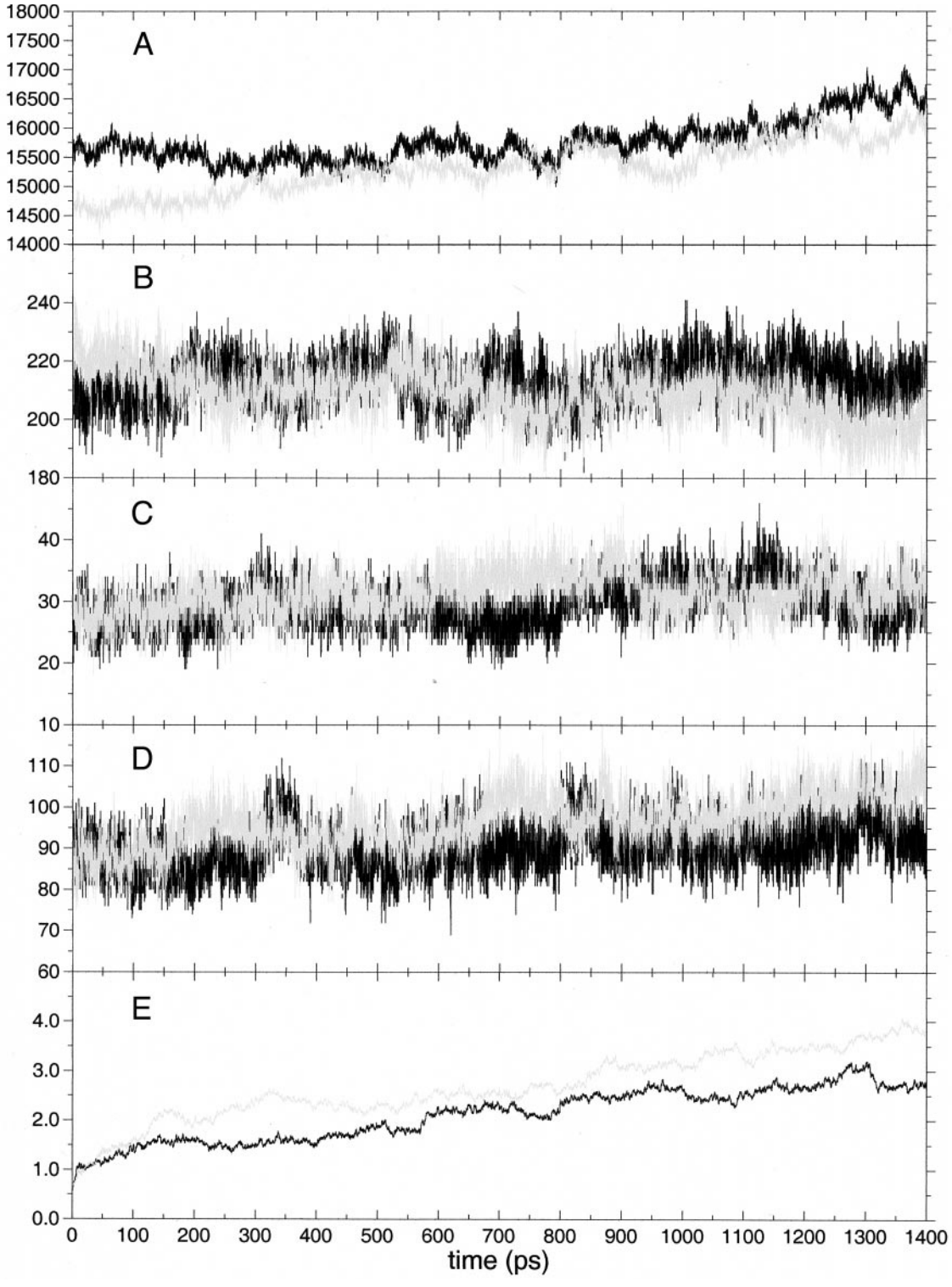

FIGURE 5 Time dependence of wild-type (*dark gray line*) and mutant (*light gray line*) PSOD geometrical properties obtained from the MD simulation trajectories: (*A*) total solvent accessible surface area of the protein dimer (E^2); (*B*) number of backbone's hydrogen bonds; (*C*) number of residues exploring unfavourable regions of the Ramachandran plot; (*D*) number of residues in random coil conformation; (*E*) inter-subunit volume (E^3).

external crevices, measured using the SURFNET program (Laskowski, 1995), is larger in the mutant than in the native enzyme over the entire trajectory (average values are 3652.3 $Å^3$ and 3074.5 $Å^3$, respectively) (Fig. 5 *E*). This result indicates that small changes at the inter-subunit surface, such as that brought by the Val→Gly

mutation, may lead to a different dynamic behavior, and provide an explanation for the higher quenching effect of the I^- anion observed for the mutated enzyme.

Interesting information comes from the root mean square fluctuations (RMSF) of each amino acid, which are reported in Fig. 6 as a difference between the native and mutated proteins of the average value of the two subunits. The RMSF differences indicate that the dynamics of the overall protein core is identical in both the native and mutated proteins, but there are also regions in which the mobility is either increased or decreased in the mutant, when compared to the native enzyme. In particular, there are three regions with increased flexibility (around residues 50, 63, and 135), located in the two loops that define the channel controlling the active site accessibility from external molecules, and two regions with reduced mobility (around residues 83 and 110) located in the Trp83 area. The reduced mobility of Trp83 in the mutated protein can be statistically explained considering all the conformations sampled by this residue during the trajectory. As shown in Fig. 7 the Trp83 average structure for the wild-type and the mutated enzyme indicates that, as a consequence of mutation, the indole ring samples more frequently a region close to the facing subunit, partially filling the cavity created at the interface by the substitution of the native valine with glycine. The new location reached by the tryptophan side-chain in the mutant explains its reduced mobility, and causes a slight interface reorganization in which Phe81 and Pro106 approach the opposite subunit more tightly, whereas the remaining intersubunit contacts are more loose and fluctuating than in the wild-type enzyme. Actually, the MD simulation indicates that the removal of Val29 changes the shape of the intersubunit surface, creating two new cavities in the quite flat interface of the PSOD native protein, that becomes more interdigitated as observed in the eukaryotic enzymes (Getzoff et al., 1986). It is interesting to notice that the filling of the cavity by tryptophan is not observed by x-ray diffraction, even at high resolution (Stroppolo et al., 2000), but it is clearly demonstrated by MD simulation, allowing a reliable explanation for the reduced mobility observed through

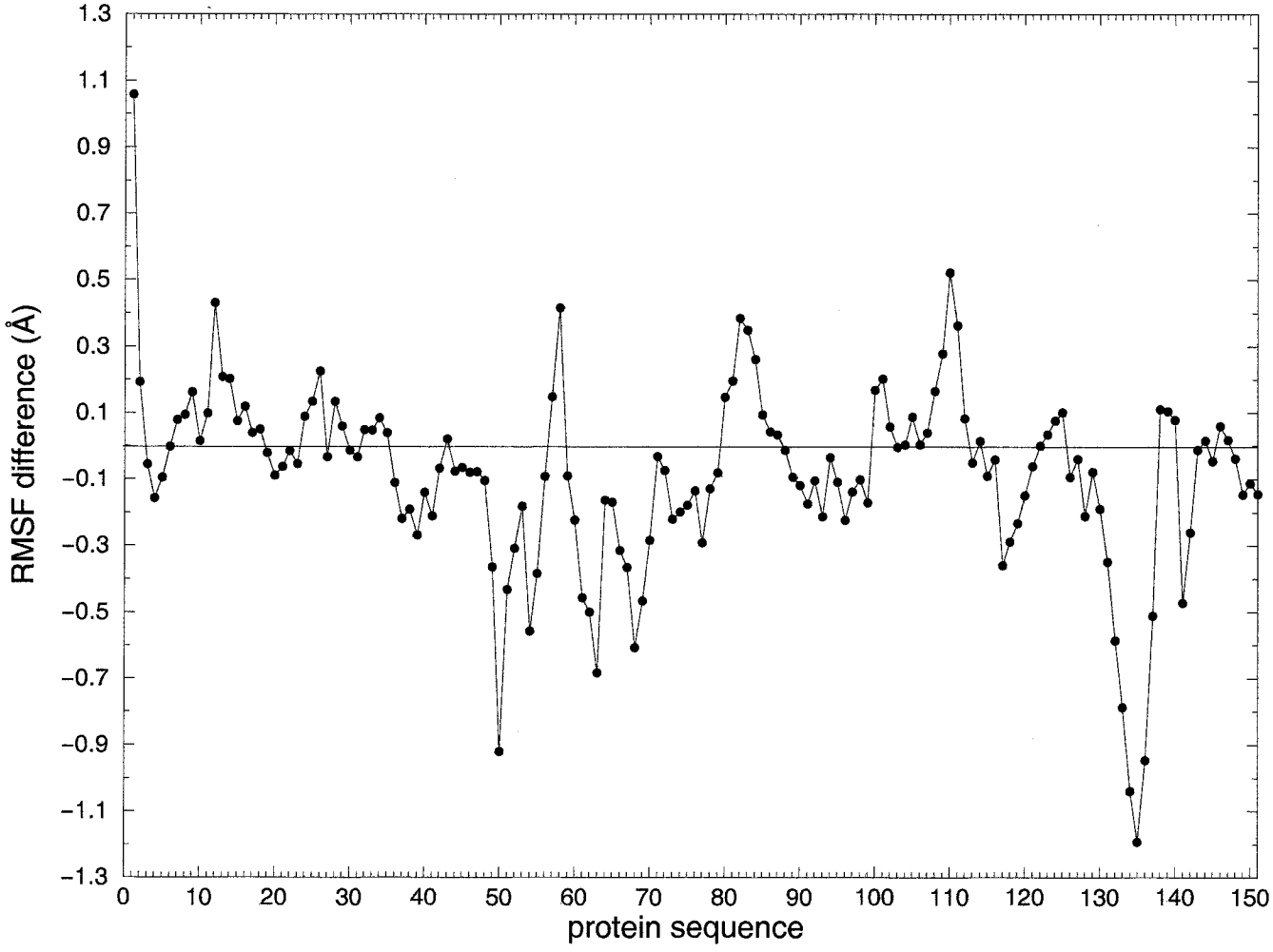

FIGURE 6 Root mean square fluctuations difference for each aminoacid between the native and mutant enzyme, averaged over the two subunits.

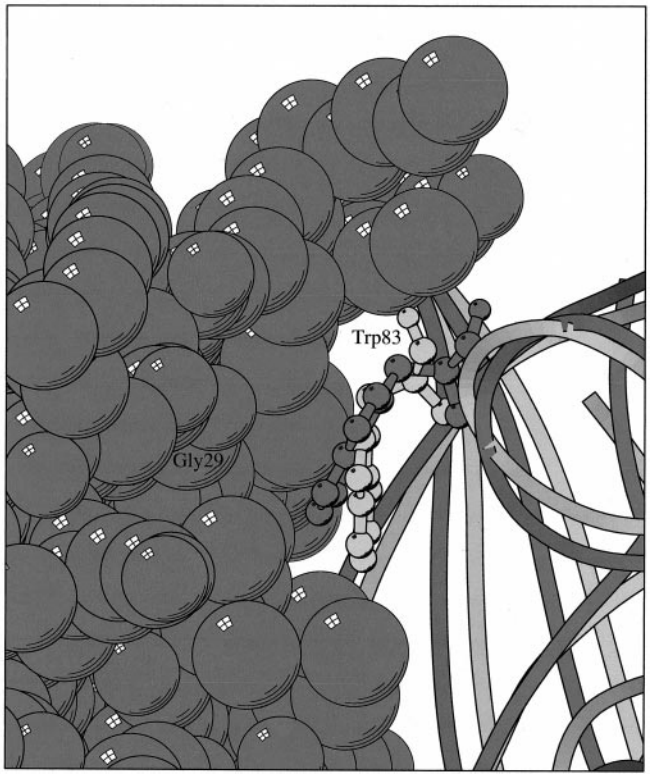

FIGURE 7 Ball-and-stick models of the Trp83 average position obtained from the MD simulation trajectory of the mutant (*dark gray*), and of the wild-type (*light gray*). The chain trace of the subunits are represented as wires using the same colors. The dark gray spacefill model represents the facing subunit of the mutant. The label "Gly29" indicates the mutation site. The picture has been obtained using the program Molscript (Kraulis, 1991).

fluorescence and phosphorescence spectroscopy. In Fig. 8, an α-chain model of PSOD is reported in which the amino acids with an RMSF difference >0.3 Å or lower than -0.3 Å, and so, having a lower or higher mobility in the mutant, are represented as blue or red spheres respectively. The figure clearly shows that, in the mutant, the residues belonging to the regions with increased rigidity are located at the inter-subunit surface in the Trp83 area, whereas the residues belonging to the three regions having an increased flexibility (one in the loop 7, 8 and two in the S-S subloop of loop 6, 5) are delimiting the active site. The overall protein core, corresponding to the β-barrel, has comparable fluctuations in both the native and mutated enzyme. From this picture it can be estimated that in the mutant the coupling between the two subunits may transduce flexibility to the active site loops through a more rigid inter-subunit interface, as already suggested in previous MD simulations of eukaryotic SOD (Falconi et al., 1996; Chillemi et al., 1997; Falconi et al., 1999).

Support to this hypothesis comes from the dynamic cross-correlation matrices which permit us to distinguish amino acid residues with correlated motions. Fig. 9 A and B show the presence of correlated motions between residues located in the two subunits. In these plots a black square is reported when the correlation between two amino acid residues is greater than 0.5 Å, while a gray square is reported if the correlation is lower than this value. Inspection of Fig. 9 *A* and *B* reveals an interesting behavior, in fact in the native protein there are few inter-subunit correlations and the two monomers behave as almost independent units (Fig. 9 *A*). On the other hand, a broad pattern of inter-subunit correlations is found in the mutated protein indicating that the single Val→Gly mutation is sufficient to change the inter-subunit communication in PSOD (Fig. 9 *B*). Closer inspection of the matrices indicates that the slight inter-subunit correlation presents in the wild-type enzyme is extended in the mutant. In detail, there are two well defined groups of

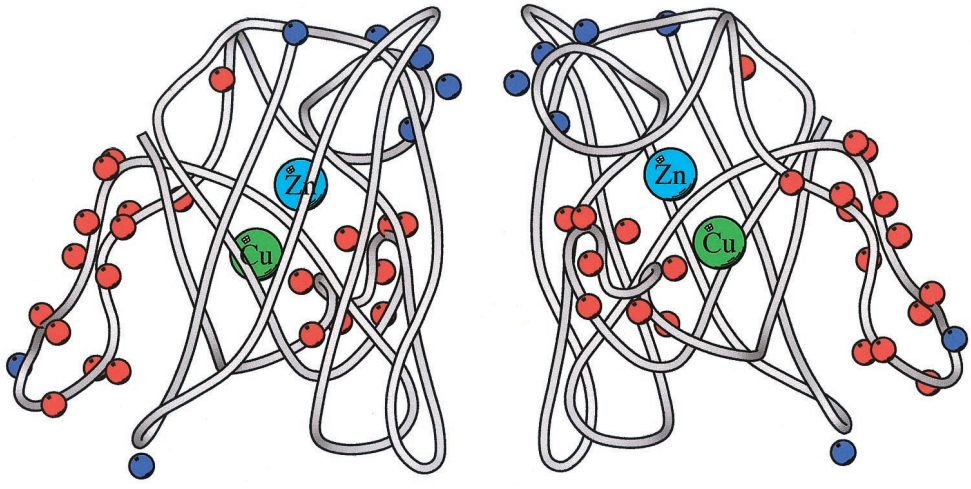

FIGURE 8 Thin wire representation of the wild-type PSOD fold. Blue spheres represent the location of aminoacids having an RMSF difference between wild-type and mutant PSODs >0.3 Å, and red spheres represent the location of aminoacids having an RMSF difference <-0.3 Å. The labeled spheres represent the metal ions. This picture has been obtained using the program Molscript (Kraulis et al., 1991).

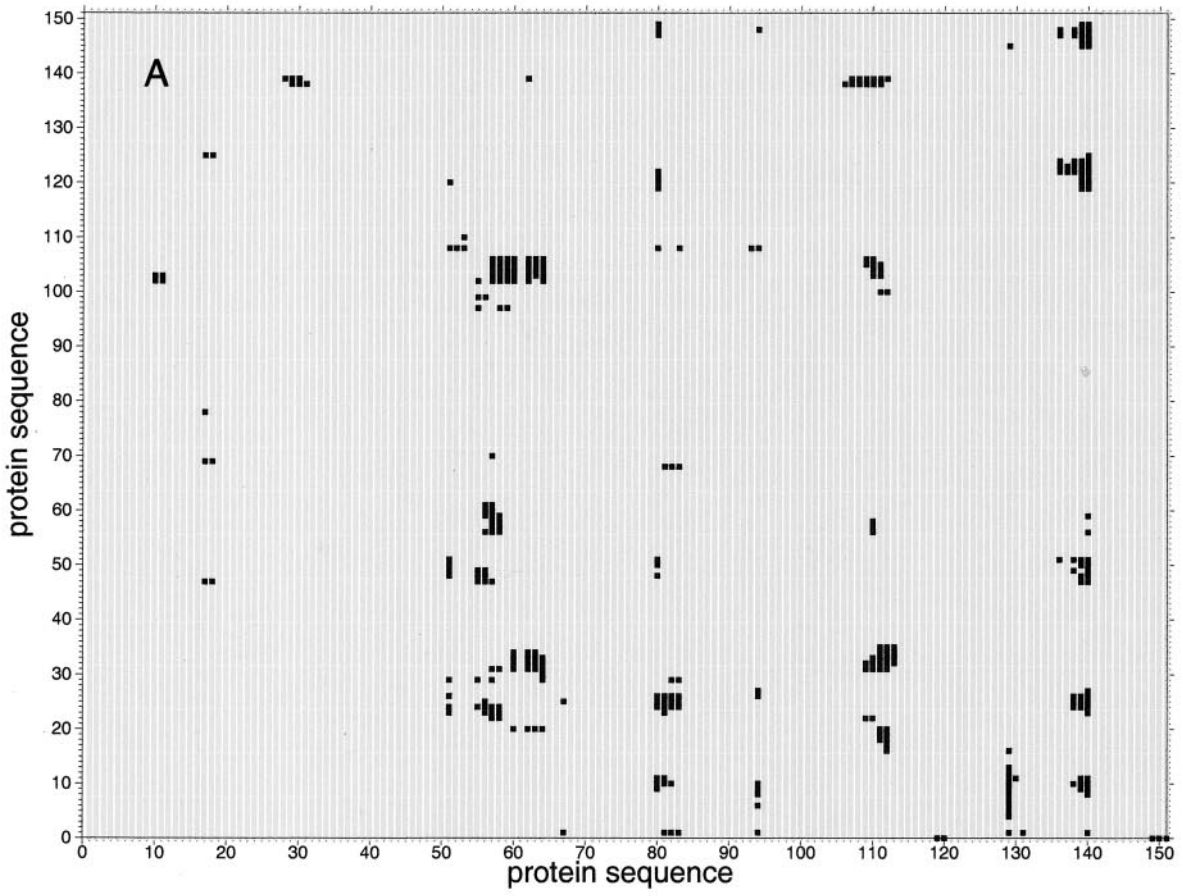
A
protein sequence
protein sequence
0
10
20
30
40
50
60
70
80
90
100
110
120
130
140
150

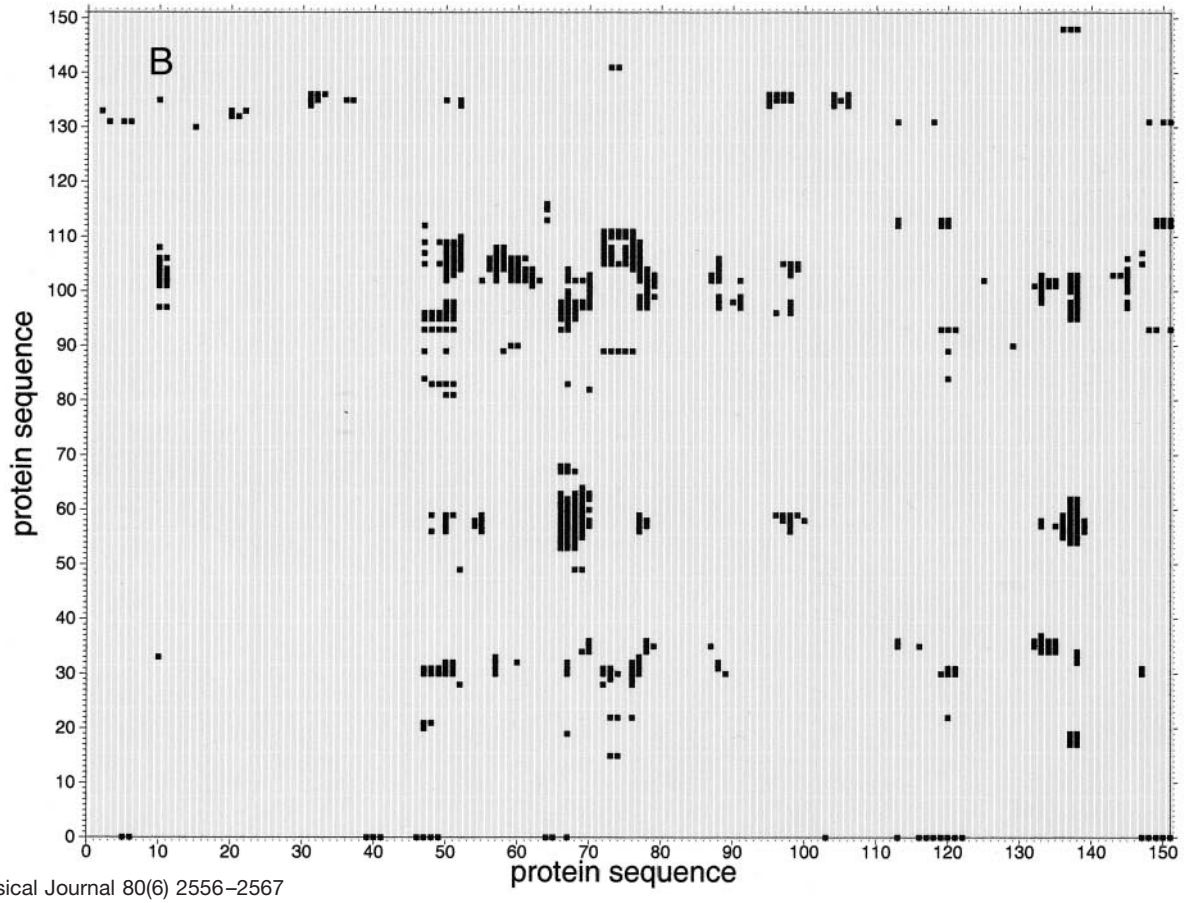
B
protein sequence
protein sequence
0
10
20
30
40
50
60
70
80
90
100
110
120
130
140
150

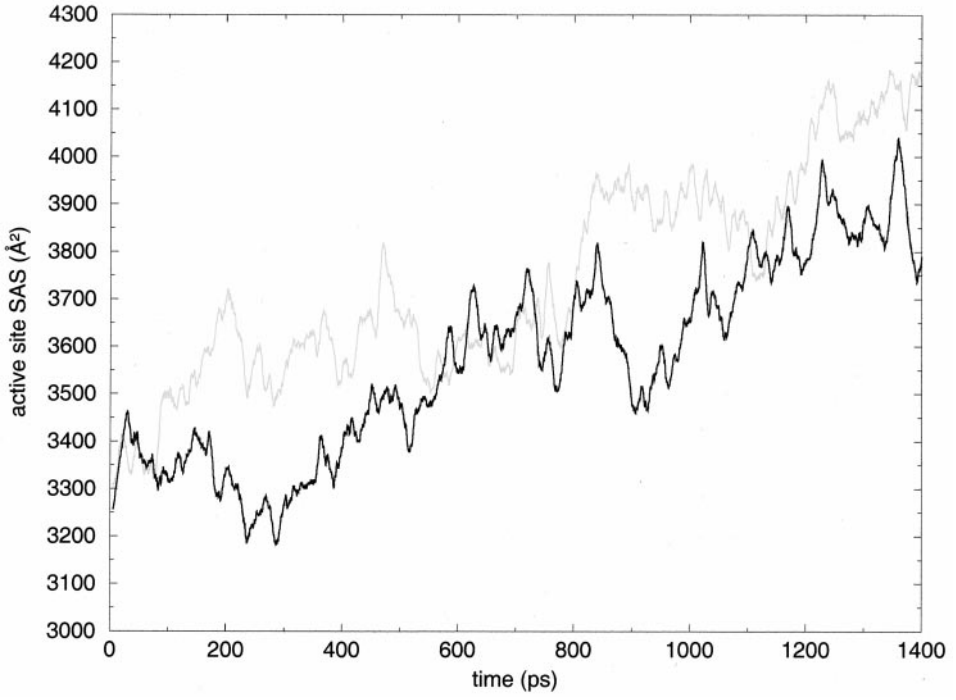

FIGURE 10 Average solvent accessible active sites surface area of wild-type (*black line*) and mutant enzyme (*gray line*).

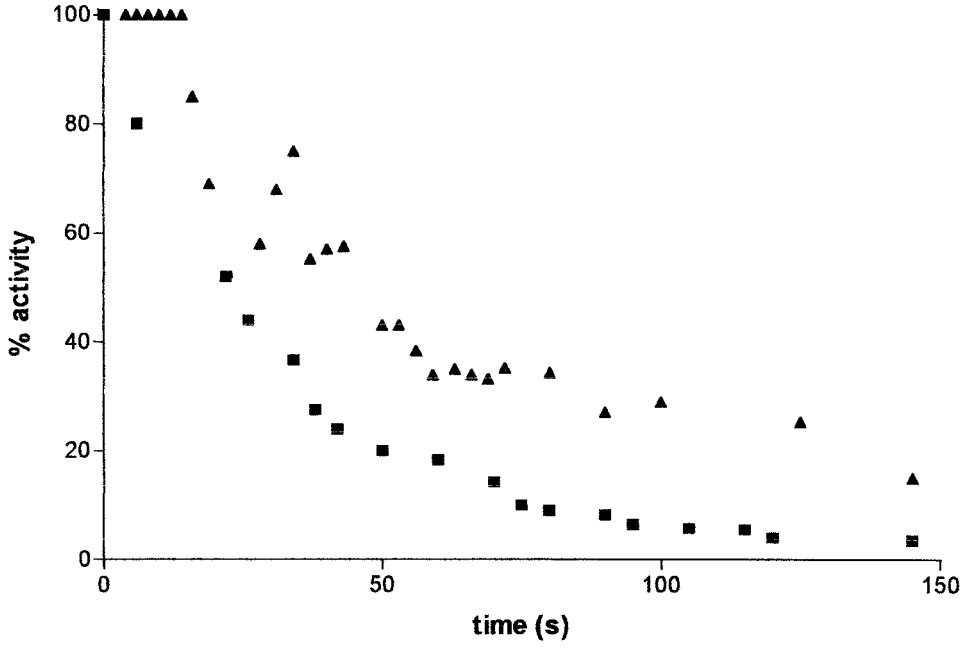

FIGURE 11 Percentual superoxide dismutase activity as function of time observed upon incubating the protein with 0.1 mM EDTA at 37°C. Wild-type (▲), Val29→Gly ■) Cu, Zn PSOD. The enzyme was 1.25×10^{-6} M in 20 mM Tris HCl (pH 7.0), 0.1 mM EDTA. Superoxide dismutase activity was detected through the pyrogallol method (Marklund and Marklund, 1974), following the absorbance increase at 420 nm.

FIGURE 9 A and B. Dynamic inter-subunits cross-correlation map calculated for the wild-type (*A*) and the mutant (*B*) Cu, Zn PSOD dimers. The black squares represent $0.5 < c_{ij} < 1.0$ and the gray squares represent $0.0 < c_{ij} < 0.5$ (c_{ij} is defined in Eq. 1 of Materials and Methods).

amino acids which display an high degree of correlation. The first set of correlated motions occurs between interface residues of β-strand 4f of one monomer (residues 105 to 111), and residues forming the active site S-S sub-loop of the other monomer (residues 50 to 70 of loop 6, 5), while the second set occurs between residues forming the active site S-S sub-loops belonging to the different monomers (residues 50 to 70 of loop 6, 5), confirming that interface mutation can transduce specific motions in the regions located in proximity of the active site.

It is interesting to note that the mutation site shows identical dynamics in both the mutant and the wild-type enzyme as evidenced by its RMSF (Fig. 6), while differences are observed at the level of the amino acids facing the mutated residue. This region become more rigid in the mutant allowing a direct mechanical coupling between the two subunits that is then transduced toward the most flexible regions of the proteins, i.e., the loops surrounding the active site, which become more mobile. In particular, the increased rigidity of the Trp83 residue, located in the Zn sub-loop of loop 6,5 and embedded in the hole generated by the Val29→Gly substitution, allows a mechanical coupling through the Zn sub-loop to the S-S sub-loop of loop 6,5, surrounding the active copper. This coupling induces larger fluctuations of the S-S sub-loop, which generate an easier accessibility of the copper atom to the substrate, increasing the substrate-copper association rate and then the enzymatic second order catalytic rate.

Evidence for increased active metal accessibility also comes from a plot of the solvent accessible surface (Connolly, 1983) of the active sites. The solvent accessible surface is defined as the accessibility of the atoms enclosed in a 15.0 Å radius sphere from the copper atom, computed for each PSOD configuration and averaged over the two subunits. This sphere includes the metals, all the ligand amino acids, the active site arginine and some loop residues belonging to the active site border. The plot in Fig. 10 indicates that the active site solvent accessible surface, which is the same in the two enzymes when measured in the structures obtained through x-ray diffraction (Stroppolo et al., 2000), reaches a higher average value in the mutant during the simulation, confirming a greater dynamic copper accessibility for external agents.

Activity loss measurements

Further evidence for an increased copper accessibility to external agents comes from activity measurements carried out, using the pyrogallol method, as a function of time in presence of 0.1 mM EDTA at 37°C. Such an experiment, reported in Fig. 11, detects the ability of EDTA to remove the copper from the enzyme. The plot indicates that loss of copper is faster in the mutant than in the native enzyme, a finding that can be explained considering an higher copper accessibility in the mutant enzyme. We want to stress that the increased copper accessibility is not simply a static effect, because x-ray diffraction at high resolution (Stroppolo et al., 2000) did not show any structural difference, but must be correlated to the larger fluctuations of the mutated enzyme, i.e., to its dynamic properties. Mutation at the interface makes the copper more accessible to external agents such as EDTA.

CONCLUSIONS

Here we report a clear example of dynamics/function correlation in an enzyme. This finding is of general interest because, although this phenomenon is quite well accepted, there are still only a few examples of unequivocal dynamics/function relationship. In this example, a single amino acid mutation of a residue located at the dimer interface induces a twofold increase of the catalytic rate of PSOD (Stroppolo et al., 2000). This mutation does not produce structural changes detectable by x-ray diffraction (Stroppolo et al., 2000), but generates, when compared to the wild-type, an enhancement of the mechanical coupling between the two subunits, which transduces higher fluctuations to the loops proximal to the active site modulating the metal reactivity and stability. From a specific point of view, the biological relevance of this work relies on the fact that the loss of zinc from either wild-type or mutant Cu, Zn SODs, associated with amyotrophic lateral sclerosis, induces apoptosis in cultured motor neurons (Crow et al., 1997) and that metal mobility may be modulated by mutation far from the active site. From a more general point of view this work indicates that, in the post-genome era, the effort to understand the functional role of each macromolecule, encoded by a specific sequenced gene (Eisemberg et al., 2000), must not only be devoted to solve its structure, but must be extended to a complete description of its dynamic properties.

This work was supported in part by a MURST COFIN 2000 project.

REFERENCES

Allen, M. P., and D. J. Tildesley. 1987. Computer Simulation of Liquids. Clarendon Press, Oxford.

Battistoni, A., S. Folcarelli, L. Cervoni, F. Polizio, A. Desideri, A. Giartosio, and G. Rotilio. 1998. Role of the dimeric structure in Cu, Zn superoxide dismutase. pH-dependent, reversible denaturation of the monomeric enzyme from Escherichia coli. *J. Biol. Chem.* 273:5655–5661.

Berendsen, H. J. C., J. R. Grigera, and T. P. Straatsma. 1987. The missing term in effective pair potentials. *J. Phys. Chem.* 91:6269–6271.

Berman, H. M., J. Westbrook, Z. Feng, G. Gilliland, T. N. Bhat, H. Weissig, I. N. Shindyalov, and P. E. Bourne. 2000. The Protein Data Bank. *Nucleic Acids Res.* 28:235–242.

Bordo, D., D. Matak, K. Djinovic-Carugo, C. Rosano, A. Pesce, M. Bolognesi, M. E. Stroppolo, M. Falconi, A. Battistoni, and A. Desideri. 1999. Evolutionary constraints for dimer formation in prokaryotic Cu, Zn superoxide dismutase. *J. Mol. Biol.* 285:283–296.

Bordo, D., A. Pesce, M. Bolognesi, M. E. Stroppolo, M. Falconi, and A. Desideri. 2001. Cu, Zn superoxide dismutase in prokaryotes and eukaryotes. *In* Handbook of Metalloproteins, K.Wieghardt, R. Huber, T. Poulos, and A. Messerschmidt, editors. John Wiley and Sons, Ltd. London. In press.

Bourne, Y., S. M. Redford, H. M. Steinman, J. R. Lepock, J. A. Tainer, and E. D. Getzoff. 1996. Novel dimeric interface and electrostatic recognition in bacterial Cu, Zn superoxide dismutase. *Proc. Natl. Acad. Sci. U.S.A.* 93:12774–12779.

Calabrese, L., D. Cocco, L. Morpurgo, B. Mondovi, and G. Rotilio. 1976. Cobalt bovine superoxide dismutase. Reactivity of the cobalt chromophore in the copper-containing and in the copper-free enzyme. *Eur. J. Biochem.* 64:465–470.

Chillemi, G., M. Falconi, A. Amadei, G. Zimatore, A. Desideri, and A. Di Nola. 1997. The Essential Dynamics of Cu, Zn superoxide dismutase: suggestion of intersubunit communication. *Biophys. J.* 73:1007–1018.

Cioni, P., E. Gabellieri, M. Gonnelli, and G. B. Strambini. 1994. Heterogeneity of protein conformation in solution from the lifetime of tryptophan phosphorescence. *Biophys. Chem.* 52:25–34.

Cioni, P., and G. B. Strambini. 1998. Acrylamide quenching of protein phosphorescence as a monitor of structural fluctuations in the globular fold. *J. Am. Chem. Soc.* 120:11749–11757.

Connolly, M. L. 1983. Solvent accessible surfaces of protein and nucleic acids. *Science.* 221:709–713.

Crow, J. P., J. B. Sampson, Y. Zhuang, J. A. Thompson, and J. S. Beckman. 1997. Decreased zinc affinity of amyotrophic lateral sclerosis-associated superoxide dismutase mutants leads to enhanced catalysis of tyrosine nitration by peroxynitrite. *Neurochemistry.* 69:1936–1944.

Desideri, A., M. Falconi, F. Polticelli, M. Bolognesi, K. Djinovic, and G. Rotilio. 1992. Evolutionary conservativeness of electric field in the Cu, Zn superoxide dismutase active Site. *J. Mol. Biol.* 223:337–342.

Eisemberg, D., E. M. Marcotte, I. Xenarios, and T. O. Yeates. 2000. Protein function in the post-genomic era. *Nature.* 405:823–826.

Falconi, M., E. Paci, and R. Gallimbeni. 1996. Dimer Asymmetry in Superoxide Dismutase studied by Molecular Dynamics Simulation. *J. Comput-Aided Mol. Design.* 10:490–498.

Falconi, M., F. Venerini, and A. Desideri. 1999. Dependence of the mechanical intersubunit communication of a dimeric protein to specific mutations as revealed by molecular dynamics simulation. *J. Mol. Liq.* 84:29–37.

Folcarelli, S., F. Venerini, A. Battistoni, P. O'Neill, G. Rotilio, and A. Desideri. 1999. Toward the engineering of a super efficient enzyme. *Biochem. Biophys. Res. Commun.* 256:425–428.

Foti, D., B. Lo Curto, G. Cuzzocrea, M. E. Stroppolo, F. Polizio, M. Venanzi, and A. Desideri. 1997. Spectroscopic characterization of recombinant Cu, Zn superoxide dismutase from *Photobacterium leiognathi* expressed in *Escherichia coli*: evidence for a novel catalytic copper binding site. *Biochemistry.* 36:7109–7113.

Gabellieri, E., S. Rahuel-Clermont, G. Branlant, and G. B. Strambini. 1996. Effects of NAD^+ binding on the luminescence of tryptophan 84 of Glyceraldehyde-3-phosphate dehydrogenase from *Bacillus stearothermophilus. Biochemistry.* 35:12549–12559.

Getzoff, E. D., J. A. Tainer, and A. J. Olson. 1986. Recognition and interactions controlling the assemblies of beta barrel domains. *Biophys. J.* 49:191–206.

Hershberger, M. V., A. H. Maki, and W. C. Galley. 209. 1980. Phosphorescence and optically detected magnetic resonance studies of a class of anomalous tryptophan residues in globular proteins. *Biochemistry.* 19: 2204–2.

Kabsch, W., and C. Sander. 1983. Dictionary of protein secondary structure: pattern recognition of hydrogen-bonded and geometrical features. *Biopolymers.* 22:2577–2637.

Kay, L. E. 1998. Protein dynamics from NMR. *Nature Struct. Biol.* 5(Suppl):513–517.

Klapper, I., R. Hagstrom, R. Fine, K. Sharp and B. Honig. 1986:Focusing of electric fields in the active site of Cu-Zn superoxide dismutase: effects of ionic strength and amino-acid modification. *Proteins.* 1:47–59.

Kohen, A., R. Cannio, S. Bartolucci, and J. P. Klinman. 1999. Enzyme dynamics and hydrogen tunnelling in a thermophilic alcohol dehydrogenase. *Nature.* 399:496–499.

Kraulis, P. J. 1991. MOLSCRIPT: a program to produce both detailed and schematic plots of protein structures. *J. Appl. Crystallogr.* 24:946–950.

Landt, O., H. P. Grunert, and U. Hahn. 1990. A general method for rapid site-directed mutagenesis using the polymerase chain reaction. *Gene.* 96:125–128.

Laskowski, R. A. 1995. SURFNET: A program for visualizing molecular surfaces, cavities and intermolecular interactions. *J. Mol. Graph.* 13: 323–330.

Lee, W. E. 1985. Delayed emission and the heavy-atom effect as probes of biomolecular structure and dynamics. Ph.D. Thesis. McGill University, Montreal, Quebec, Canada.

Lowry, O. H., N. J. Rosebrough, A. L. Farr, and R. J. Randall. 1951. Protein measurement with the Folin-Phenol reagents. *J. Biol. Chem.* 193:265–275.

Malvezzi-Campeggi, F., M. E. Stroppolo, G. Mei, N. Rosato, and A. Desideri. 1999. Evidence of stable monomeric species in the unfolding of Cu, Zn superoxide dismutase from Photobacterium leiognathi. *Arch. Biochem. Biophys.* 370:201–207.

Marklund, S., and G. Marklund. 1974. Involvement of the superoxide anion radical in the autoxidation of pyrogallol and a convenient assay for superoxide dismutase. *Eur. J. Biochem.* 47:469–474.

McCammon, J. A.,. and S. C. Harvey. 1987. Dynamics of Proteins and Nucleic Acids. London, Cambridge University Press.

Melchionna, S., and G. Ciccotti. 1997. Atomic stress isobaric scaling for systems subjected to holonomic constraints. *J. Chem. Phys.* 106: 195–200.

Melchionna, S., A. Luise, M. Venturoli, and S. Cozzini. 1998. DLPROTEIN: a molecular dynamics package to simulate biomolecules. *In* Science and Supercomputing at CINECA - 1997 report. M. Voli, editor. Supercomputing Group, CINECA. 496–505.

O'Neill, P., S. Davies, E. M. Fielden, L. Calabrese, C. Capo, F. Marmocchi, G. Natoli, and G. Rotilio. 1988. The effects of pH and various salts upon the activity of a series of superoxide dismutases. *Biochem. J.* 251:41–46.

Ryckaert, J. P., G. Ciccotti, and H. J. C. Berendsen. 1977. Numerical integration of the cartesian equations of motions of a system with constraints: molecular dynamics of N-alkanes. *J. Comp. Phys.* 23: 327–341.

Sergi, A., M. Ferrario, F. Polticelli, P. O'Neill, and A. Desideri. 1994. Simulation of superoxide-superoxide dismutase association rate for six natural variants: comparison with the experimental catalytic rate. *J. Phys. Chem.* 98:10554–10557.

Sines, J. J., S. A. Allison, and J. A. McCammon. 1990. Point charge distributions and electrostatic steering in enzyme/substrate encounter: Brownian dynamics of modified Copper/Zinc superoxide dismutases. *Biochemistry.* 29:9403–9412.

Smith, W., and T. R. Forester. 1996. DL POLY 2.0: A general-purpose parallel molecular dynamics simulation package. *J. Mol. Graph.* 14: 136–141.

Strambini, G. B., and M. Gonnelli. 1985. The indole nuclens triplet-state lifetime and its dependence on solvent microviscosity. *Chem. Phys. Lett.* 115:196–200.

Strambini, G. B., and M. Gonnelli. 1995. Tryptophan phosphorescence in fluid solution. *J. Am. Chem. Soc.* 117:7646–7651.

Stroppolo, M. E., A. Pesce, M. Falconi, P. O' Neill, M., Bolognesi, and A. Desideri. 2000. Single mutation at the intersubunit interface confers extra efficiency to Cu, Zn superoxide dismutase. *FEBS Letters.* 483: 17–20.

van Gunsteren, W. F., and H. J. C. Berendsen. 1987. GROMOS Manual (University of Groningen, Groningen).